

A Visco-hyperelastic Model for Prediction of the Brain Tissue Response and the Traumatic Brain Injuries

Hossein Ashrafi, M. Shariyat¹

Department of Applied Design, Faculty of Mechanical Engineering, University of Kashan, ¹Department of Applied Design, Faculty of Mechanical Engineering, K. N. Toosi University of Technology, Tehran, Iran

Abstract

Introduction: Numerous geometrically simplified models may be found in the literature on simulation of the traumatic brain injuries due to the increased intracranial pressure induced by severe translational accelerations of the brain inside the cranium following the impact waves. While numerous researchers have utilized viscoelastic models, some have employed specific hyperelastic models for behavior analysis of the brain tissue. No research has been presented so far based on the more realistic visco-hyperelastic model. **Materials and Methods:** In the present research, a realistic finite element model and four visco-hyperelastic constitutive models (viscoelastic models on the basis of the polynomial, Yeoh, Arruda-Boyce, and Ogden hyperelastic models) are employed to accomplish the outlined task. Therefore, the main motivation of the present research is checking the accuracy of the modeling procedure rather than presenting clinical results. In this regard, a realistic skull-brain model is constructed in CATIA computer code based on the magnetic resonance imaging scans and optimized in the HYPERMESH finite element software. **Results:** Influence of the contact and nonlinear characteristics of the brain tissue are considered in the simulation of the relative motions in LS-DYNA software to predict time histories of the acceleration and the coup and countercoup pressures by means of ANSYS finite element analysis software. **Discussion:** Comparing results of the four proposed visco-hyperelastic constitutive models with the available experimental reveals that employing Arruda-Boyce or Ogden-type viscoelastic models may lead to inaccurate or even erroneous results.

Keywords: Brain tissue, intracranial pressure, traumatic brain injuries, visco-hyperelastic finite element model

INTRODUCTION

The relative translational motions of the brain due to severe accelerations and decelerations, lead to increased intracranial pressure gradients on the brain tissue, cerebrospinal fluid (CSF), and the brain's blood supply vessels. The resulting pressures gradients can lead to traumatic brain injuries, blood vessels damages, and restricting blood flow to the brain and brain trauma, and consequently, to fatal conditions if the pressure exceeds 40 mmHg in adult persons.^[1] The relative motions of the brain with respect to the skull, striking and bouncing of the parenchyma against the inner skull protrusions, cavitation phenomena induced by negative pressures, and rupture of the bridging veins, axonal fibers, and vascular tissue are among the frequent origins of the damages.^[2,3] Yue *et al.*^[4,5] studied dynamic characteristics of the human skull-dura mater system and deformations of the human skull due to variations in the intracranial pressure, using a hollow sphere finite element model. The skull was simulated by a

thin-walled composite shell, and Maxwell's viscoelasticity model was employed for the human skull-dura mater. The important mechanical characteristics of the cancellous bone and dura mater is viscoelasticity.^[6,7] Willinger *et al.*^[8] and Ding *et al.*^[9] determined mechanical properties and characteristics of the compact bone, cancellous bone, and dura mater.

The early finite element models for the skull/brain complex were presented based on a simple fluid-filled spherical shell. Zhang *et al.*,^[10] Willinger *et al.*,^[11] Kleiven and von Holst,^[12] and Horgan and Gilchrist^[13] have recently developed more complicated three-dimensional (3D) models based on anatomical drawings and medical images, such as computed tomography (CT) and magnetic resonance imaging (MRI) scans. Liu *et al.*^[14] employed a transparent physical head

Address for correspondence: Dr. Hossein Ashrafi, Faculty of Mechanical Engineering, University of Kashan, Kashan, Iran. E-mail: hashrafi@kashanu.ac.ir, hhashrafi@gmail.com

Access this article online

Quick Response Code:



Website:
www.archtrauma.com

DOI:
10.4103/atr.atr_9_17

This is an open access article distributed under the terms of the Creative Commons Attribution-NonCommercial-ShareAlike 3.0 License, which allows others to remix, tweak, and build upon the work non-commercially, as long as the author is credited and the new creations are licensed under the identical terms.

For reprints contact: reprints@medknow.com

How to cite this article: Ashrafi H, Shariyat M. A Visco-hyperelastic model for prediction of the brain tissue response and the traumatic brain injuries. Arch Trauma Res 2017;6:41-8.

model with air bubbles to study the brain cavitation phenomenon in a head deceleration impact. The transparent skull model was generated based on a real human skull through a turnover formwork technique, and a transparent gel was used to represent the brain tissue. Recently, Chen and Ostoja-Starzewski^[15] presented a 3D finite element model for the human head that accounts for the important geometric characteristics of the various components within the human head, through using an efficient MRI voxel-based mesh generation method. El Sayed *et al.*^[2] presented a biomechanical model for simulation of the traumatic brain injury and damages of the soft tissues to simulate the axonal damage and cavitation injury through inelastic deformations due to frontal and oblique head impacts with external objects. The material response was divided into elastoplastic and viscoelastic components, including rate effects, shear and porous plasticity, and finite viscoelasticity.

Some researches have considered simple hyperelastic or finite viscoelastic models.^[16-22] Elastic and hyperelastic properties of the brain gray and white matters were characterized by Kaster *et al.*,^[23] based on the force-displacement data of the tissues for 25 different brain samples, using an indentation apparatus, and the material properties of the Polynomial, Yeoh, Arruda-Boyce, and Ogden hyperelastic models were obtained. Recently, Post *et al.*^[24] studied effects of loadings with an identical area beneath the curves, on the time history of the resulting von Mises stress and maximum principal strain as measures of the brain tissue damage.

In the present paper, several visco-hyperelastic finite element models are presented for simulation of the traumatic brain injuries due to the increased intracranial pressure caused by severe translational accelerations and decelerations. In this regard, a realistic skull-brain model based on the MRI is created in CATIA modeling software and optimized in HYPERMESH finite element computer code. Influence of the contact and nonlinear characteristics of the brain tissues are considered in the simulation of the relative motions in LS-DYNA software. Finally, time histories of the acceleration and the pressures are determined based on ANSYS finite element analysis software. In this regard, results of various visco-hyperelastic constitutive models are studied and compared with each other and with the available experimental results.

GEOMETRIC AND FINITE-ELEMENT MODELING

The skull is composed of a braincase (neurocranium) and a facial skeleton (splanchnocranium, viscerocranium), both sharing the base of the skull, which descends obliquely backward [Figure 1].

The cerebrum is the highest and biggest region of the brain that covers the majority of the portions of the brain. Almost all of the skull space is filled by cerebrum that is composed of the right and left cerebral hemispheres, and several bilateral gray nuclei (basal ganglia). These two parts are separated at all sections, but in some inside regions, they have little

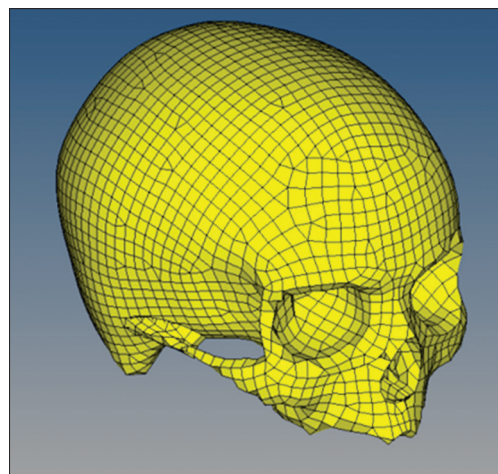


Figure 1: Finite-element model of the human skull

connections by some white fibers. The cerebral hemisphere consists of an outer gray cortical layer and an inner white core composed mainly of nerve fibers. The CSF is a clear fluid, which fills the whole subarachnoid space and acts as a protective fluid cushion around the brain and the spinal cord and damps the externally imposed shocks.

The realistic brain model is constructed based on the MRI of the brain and cranium which some of them are shown in Figure 2.^[25] The whole scan set consists of 55 parallel sections. The 3D geometric and finite element models were reconstructed based on the axial MRI available in “The Whole Brain Atlas” of Harvard Medical School.^[26] In the present research, each section is defined by many key points; so that, the assembly of the whole sections of the brain have constituted clouds of key points. The geometric model of the brain tissue is constructed in CATIA computer code, through passing surfaces through the key points of the clouds associated with each individual matter of the brain to form the whole brain model. It is known that each closed surface is identified as a volume in the computer-aided design software, for example, CATIA computer code. The reader may also refer to a book by Saba^[27] on image principles of the brain, for more details. The finite element model [Figure 3] is constructed in HYPERMESH finite element software to obtain elements with optimized topologies. The resulting finite element model includes the: (1) CSF in the form of a 3-mm thick layer, (2) gray matter, (3) white matter, (4) cerebellum, (5) corpus callosum, (6) telencephalic nuclei, (7) brain stem, and (8) ventricles. The whole assembly is illustrated in Figure 4.

10-noded second-order tetrahedral composite elements whose material properties are similar to those of the Wayne State Brain Injury Model,^[26] are employed to discretize the model. The 3 (mm) gap between the inner surface of the cranium and the outer surface of the brain is filled with the CSF. Due to the complexity of the geometries, the general contact constraint is defined between these three media and the dynamic simulation is accomplished in LS-DYNA software.

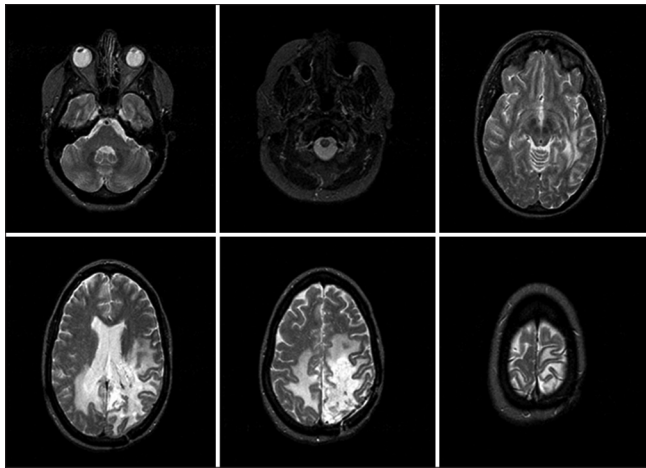


Figure 2: Magnetic resonance imaging scans of the brain and cranium.^[2]

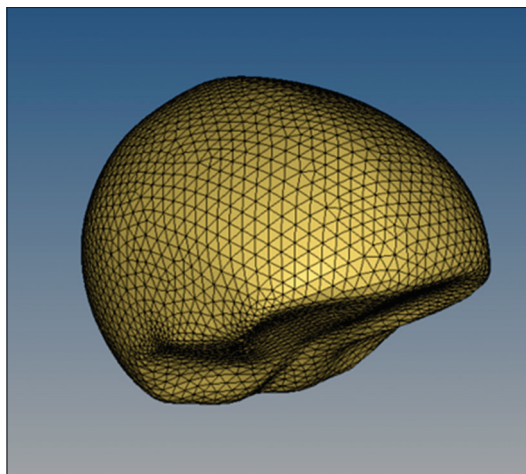


Figure 3: The full-finite element model of the human brain

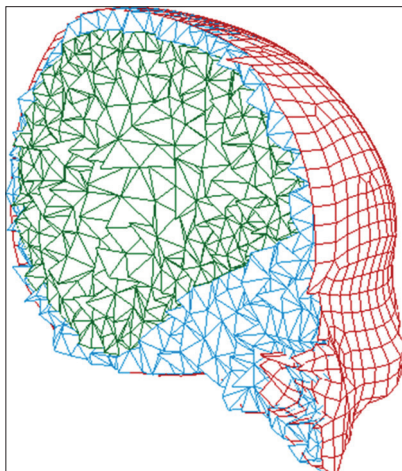


Figure 4: The skull-brain finite element assembly constructed in HYPERMESH software

DESCRIPTION OF THE MATERIAL PROPERTIES

Mechanical properties of the human skull and the CSF are listed in Table 1. Based on the studies performed on

Table 1: Material properties of the cranium and cerebrospinal fluid

Property	Skull	CSF
Mass density (kg/m ³)	1210	1004
Shear modulus μ (kPa)	3280	0.50
Bulk modulus κ (kPa)	4760	2190

CSF: Cerebrospinal fluid

deformations of the brain tissue under impact loading, it has been observed that these tissues exhibit hyperelastic behaviors.^[16-22] Hyperelasticity refers to a constitutive response that is derivable from an elastic potential function $W^{(e)}$ and is typically used for nearly incompressible materials which experience nonlinear large elastic deformations such as rubber and some biological materials. When the strain energy density function per unit

undeformed volume is defined, one may determine the stress-strain expressions from:

$$S_{ij} = \frac{\partial W^{(e)}}{\partial E_{ij}} = 2 \frac{\partial W^{(e)}}{\partial C_{ij}} = 2 \left[\frac{\partial W}{\partial I_1} \frac{\partial I_1}{\partial C_{ij}} + \frac{\partial W}{\partial I_2} \frac{\partial I_2}{\partial C_{ij}} + \frac{\partial W}{\partial I_3} \frac{\partial I_3}{\partial C_{ij}} \right] \quad (1)$$

Where S_{ij} , E_{ij} , C_{ij} , and (I_1, I_2, I_3) are components of the second Piola–Kirchhoff stress tensor, components of the Lagrangian strain tensor, components of the right Cauchy–Green deformation tensor, and the stress invariants, respectively. Several forms of the strain energy potential have been proposed for simulation of the incompressible or nearly incompressible hyperelastic materials, among them: Arruda–Boyce, Blatz–Ko, extended tube, Gent, Mooney–Rivlin, neo-Hookean, Ogden potential, polynomial form, and Yeoh models.

Evaluation of efficiency and accuracy of the hyperelastic models for the behavior and injury simulation of the skull-brain assembly is an important issue. In the present research, four well-known hyperelasticity models are adopted and modified to include the viscoelastic behaviors of the material, and their predictions are compared with the available experimental results.

Polynomial model

In this hyperelastic model, the strain energy potential is expressed by:

$$W^{(e)} = \sum_{i+j=1}^N C_{ij} (I_1 - 3)^i (I_2 - 3)^j + \sum_{k=1}^m \frac{1}{D_k} (J - 1)^{2k} \quad (2)$$

Where C_{ij} , I_1 , I_2 , I_3 , and D_k are material constants, the first and second invariants of the strain tensor, the elastic volume strain, and the material incompressibility parameter, respectively. The neo-Hookean model can be obtained by setting $n = 1$ and $C_{01} = 0$. In our comparative analyses, the second-order polynomial strain energy density function which is equivalent to the five-parameter Mooney–Rivlin

model ($n = 2$) is adopted. In this model, the initial shear and bulk moduli are defined as:

$$m = 2(C_{10} + C_{01}), K = \frac{2}{D_1} \quad (3)$$

Yeoh model

The Yeoh model^[28] is a reduced and revised form of the third-order polynomial model, wherein the strain energy potential depends on the first strain invariant only:

$$W^{(e)} = \sum_{i=1}^3 C_{i0} (I_1 - 3)^i + \sum_{k=1}^N \frac{1}{D_k} (J - 1)^{2k} \quad (4)$$

The notations are identical to those of the previous model. In this model, the initial shear and bulk moduli are defined as:

$$m = 2C_{10}, K = \frac{2}{D_1} \quad (5)$$

Arruda-Boyce model

Arruda–Boyce model depends on the first strain invariant, only and the relevant strain energy density function is:

$$W^{(e)} = m \sum_{i=1}^5 \frac{C_i}{I^{2i-2}} (I_1 - 3^i) + \frac{1}{D} \left(\frac{J^2 - 1}{2} - \ln(J) \right) \quad (6)$$

Where, $C_1 = \frac{1}{2}$, $C_2 = \frac{1}{20}$, $C_3 = \frac{11}{1050}$, $C_4 = \frac{19}{7000}$, $C_5 = \frac{519}{673750}$ λ is the locking stretch, and μ is the initial shear modulus.^[29] λ and μ are measurable parameters and:

$$K = \frac{2}{D} \quad (7)$$

Therefore, as the parameter λ tends to infinity, the model tends to the neo-Hookean model.

Ogden model

The Ogden form of the strain-energy potential density is dependent on the principal stretches of left-Cauchy strain tensor:

$$W^{(e)} = \sum_{i=1}^N \frac{m_i}{a_i} (I_1^{-a_i} + I_2^{-a_i} + I_3^{-a_i} - 3) + \sum_{k=1}^N \frac{1}{D_k} (J - 1)^{2k} \quad (8)$$

Where α_i are nondimensional exponents and λ_i are the deviatoric stretches. The first-order Ogden model depends on the two parameters that are the initial shear modulus μ and α_i . In this model, the initial shear and bulk moduli may be found from:

$$m = \frac{1}{2} \sum_{i=1}^N a_i m_i, K = \frac{2}{D_1} \quad (9)$$

The constitutive equations of the visco-hyperelastic models

The total strain tensor of the visco-hyperelastic material may be considered to be composed of hyperelastic and viscoelastic

components. Using Volterra–Boltzmann representation of the elastic behavior, one may write^[2,30-34]:

$$W^{(e)} = W_{Hyperelastic}^{(e)} + W_{Viscoelastic}^{(e)} \quad (10)$$

$$W_{Viscoelastic}^{(e)} = \sum_{j=1}^3 \sum_{r=1}^N \frac{m_j}{a_r} ([\exp(e_j)]^{a_r} - 1) + \frac{k}{2} q^2 \quad (11)$$

Where N , m_j , a_r , k , e_j , and q are the number of the required Ogden’s functions to model the shear deformations, shear moduli, dimensionless stretch component, bulk modulus, and eigenvalues of the elastic logarithmic shear strains associated with the principal stretches and logarithmic volumetric strain,^[2] respectively. $W_{Hyperelastic}^{(e)}$, that is, the strain energy density function due to the hyperelastic nature of the material per unit volume were given in equations 2, 4, 6, 8 for the considered four hyperelastic models.

Boundary conditions

In the present research, the possibility of the brain injury is investigated through simulation of the impact of the frontal region of the skull with a rigid plate. The initial velocity of the skull is assumed to be 7.5 m/s (27 km/m). Value of the initial velocity is chosen identical to that of an experiment performed by Nahum *et al.*^[35]

RESULTS AND DISCUSSIONS

In the present section, a comparative study is carried out for a better judgment about the usefulness of the visco-hyperelastic models introduced in section 3, for behavior simulation of the skull-brain system. Such comparative study has not been performed so far. The imposed boundary conditions are defined in section 4. Material properties of the adopted hyperelastic models are listed in Table 2. The viscoelastic parameters of the materials are given in Table 3.

Results of the present finite element model are compared with the experimental ones. Quadratic pyramid elements are used to discretize the visco-hyperelastic model. Convergence of the resulting finite element mesh is checked through comparing

Table 2: Material properties of the considered hyperelasticity models^[26]

Model name	Property	White tissue	Gray tissue	P
Arruda-Boyce	μ (N/m ²)	624±144	422±87	1.25e-16
	λ	1.60±0.22	1.57±0.25	0.617
Ogden	μ (kPa)	624±144	422±87	1.25e-16
	α	17.9±4.3	17.8±4.26	0.810
Yeoh	C_{10} (N/m ²)	287±69	185±40	4.26e-17
	C_{20} (N/m ²)	1002±441	601±251	4.33e-9
	C_{30} (N/m ²)	0.012±0.006	0.010±0.004	0.087
Polynomial	C_{10} (N/m ²)	101±26	7.16±14.30	1.10e-12
	C_{01} (N/m ²)	101±26	7.16±14.30	1.10e-12
	C_{11} (N/m ²)	2410±1070	1320±479	1.60e-11
	C_{20} (N/m ²)	16.3±16.8	4.59±2.55	1.05e-7
	C_{02} (N/m ²)	16.3±16.8	4.59±2.55	1.05e-7

Table 3: The viscoelastic parameters of the materials^[15]

Property	White tissue	Gray tissue
ρ (kg/m ³)	1040	1040
κ (GPa)	2.19	2.19
μ_0 (kPa)	41	3.4
μ_∞ (kPa)	7.8	6.4
α_r (/s)	700	700

results of successive refinement of the mesh; so that finally, ignorable changes in the results were noticed by further refinement of the mesh. The performed convergence study whose results are not included here to save space has revealed that choosing about 20000 elements is vital for achieving convergent results.

The experimental results include time variations of pressures of the coup and countercoup regions [Figure 5] reported by Nahum *et al.*^[35] and time history of acceleration of the center of gravity of the brain measured by Trosseille *et al.*^[36] The time histories of pressures of the coup and countercoup regions are extracted from an article by Chen and Ostojca-Starzewsky.^[15] Time-dependency of the shear modulus, due to the viscoelastic nature of the material properties, may be defined as:

$$m = m_\infty + (m_0 - m_\infty)e^{-a_r t} \quad (12)$$

Where m_0 and m_∞ are the short-term and long-term shear moduli, respectively.

Results of the visco-hyperelastic version of the polynomial, Yeoh, Arruda–Boyce, and Ogden hyperelasticity models are illustrated in Figures 6 and 7 for the coup and countercoup regions, respectively, and compared with the experimental results. Deviations of the predicted peak pressures from those of the experimental ones are given in Table 4, for various visco-hyperelastic models.

Results illustrated in Figures 6 and 7 reveal that the maximum magnitudes of the coup and countercoup pressures predicted by the polynomial visco-hyperelastic model are less than those of the experimental results. However, based on results listed in Table 4, the discrepancies between the finite element and the experimental results are lowest for the polynomial constitutive model. Moreover, curvatures of the time history graphs of the finite element and experimental results show the highest concordance; so that effects of the vacuums occurred in the coup and countercoup regions in the CSF have been simulated more accurately. Therefore, the accuracy of predictions of these models is more reliable.

On the other hand, since the polynomial visco-hyperelastic model has underestimated the coup and countercoup peak pressures, its results are not on the safe side. The peaks are slightly postponed in comparison with the experimental results. Results of Yeoh visco-hyperelastic model [Figures 7-10] are slightly greater than the experimental results. Thus, they are on the safe side. On the other hand, accuracy on these results is located in the second rank (after the polynomial

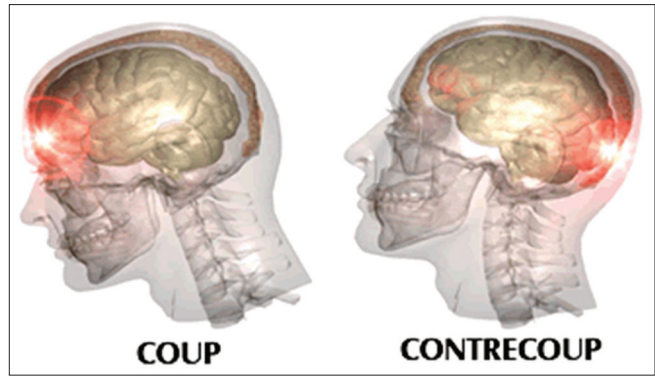


Figure 5: Different views of the coup and countercoup regions of the brain^[37]

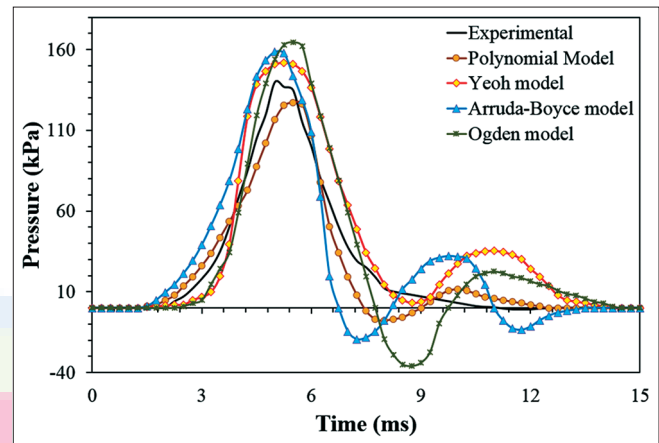


Figure 6: A comparison among time histories of the coup pressure predicted by various visco-hyperelastic models and Nahum *et al.* experimental results

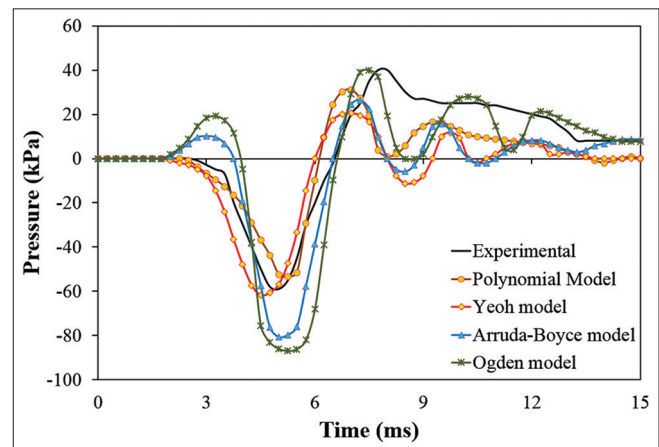


Figure 7: A comparison among time histories of the countercoup pressure predicted by various visco-hyperelastic models and Nahum *et al.* experimental results

visco-hyperelastic model). The predicted behaviors for the vacuum regions are not reliable. The peak pressures have occurred slightly before the real ones.

In Arruda–Boyce visco-hyperelastic model, occurrence times of the peak pressures are close, to a great extent, to

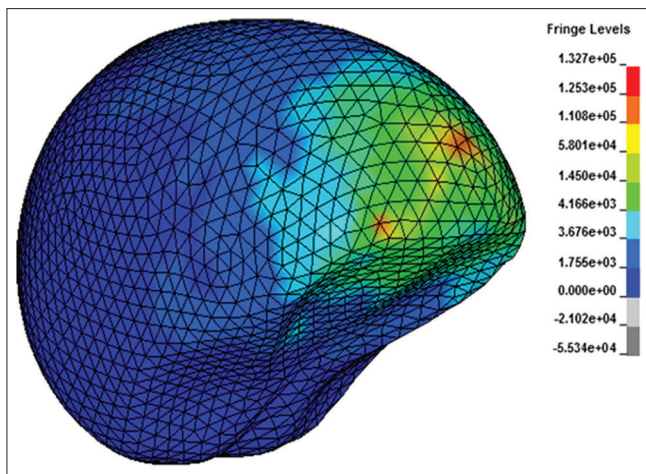


Figure 8: Distribution of the coup pressure predicted by the polynomial visco-hyperelastic model

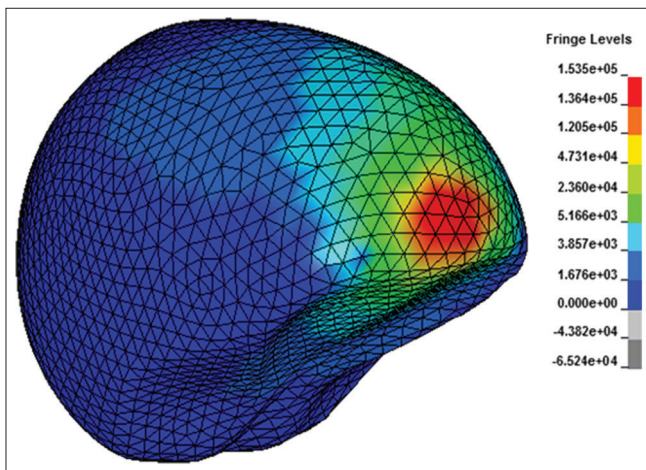


Figure 9: Distribution of the coup pressure predicted by Yeoh visco-hyperelastic model

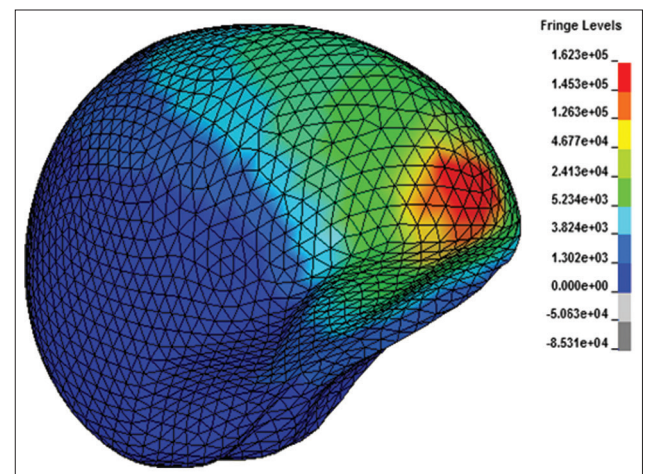


Figure 10: Distribution of the coup pressure predicted by Arruda-Boyce visco-hyperelastic model

those of the experimental ones. But as results of Table 4 confirm, discrepancies between predictions of this model

Table 4: Deviations of the peak pressures predicted by various models from Nahum *et al.* experimental results

Visco-hyperelastic model	Difference in the coup pressure (%)	Difference in the countercoup pressure (%)
Polynomial	-3.52	-6.54
Yeoh	9.33	9.89
Arruda-Boyce	14.32	43.21
Ogden	17.78	53.18

and the experimental results are significant. Magnitudes of the peak pressures predicted by this model are remarkably higher than those of the experimental ones. In comparison to the previous visco-hyperelastic models, a much oscillatory response is observed in times following the peak pressures. However, responses of this region of the time history are more consistent with the experimental results, in comparison to Yeoh model. Therefore, it may be concluded that this model does not simulate the visco-hyperelastic nature of the brain tissue accurately.

The last visco-hyperelastic model, that is, Ogden model significantly overestimates the peak pressures of both the coup and countercoup regions of the brain. Results presented in Figures 6 and 7 and results reported in Table 4 reveal that in spite of using this model by some researchers,^[2] results of this model are not reliable at all. Results of Ogden model show the greatest discrepancies with respect to the experimental results. Furthermore, redundant oscillations have appeared in the predicted responses shown in Figures 6 and 7.

However, the absolute peak of each response is the most important parameter for injury assessment of the brain tissue and the blood vessels that are in the neighborhood of the coup and countercoup regions. Therefore, the minor oscillations can be ignored in the responses. Comparing results shown in Figures 6 and 7 with experimental results reported in^[36,38,39] reveals that predictions of the polynomial model are even closer to those of the real ones.

Figures 6 and 7 reveal that the coup peak pressures are greater than those of the countercoup region. The distributions predicted for the coup pressure by the four visco-hyperelastic models are shown in Figures 8-11.

One of the discrepancy sources is the shortcoming in accurately modeling the inertial and volume characteristics. For this reason, time histories of the acceleration of the center of gravity of the brain are determined by LS-DYNA software for the various visco-hyperelastic models and plotted in Figure 12. Results of the polynomial visco-hyperelastic model show a better agreement with the time history reported by Trosseille *et al.*^[36] regarding both the peak acceleration and the peak occurrence time. Again, Ogden model has led to the worst results. Results of Yeoh model are still in the second rank. Therefore, both acceleration of the center of gravity of the brain and the pressure results have led to identical

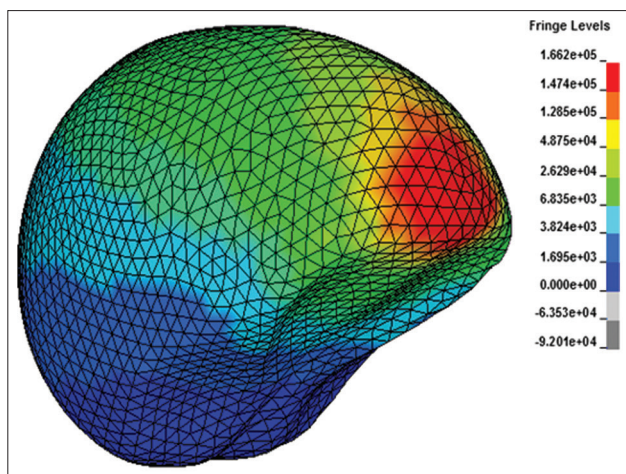


Figure 11: Distribution of the coup pressure predicted by Ogden visco-hyperelastic model

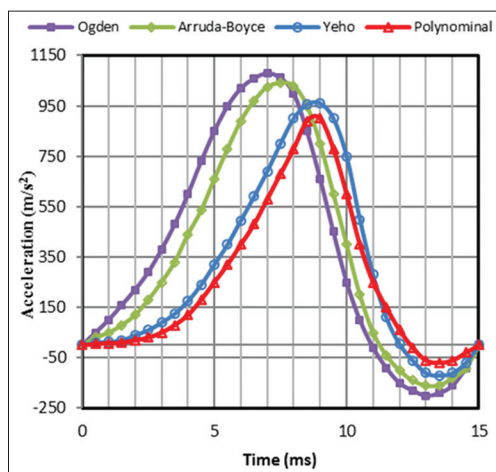


Figure 12: Acceleration of the human head at the center of gravity

conclusions that the models may be ordered with respect to the accuracy as the polynomial, Yeoh, Arruda–Boyce, and Ogden models.

Zhou *et al.*^[40] reported that the mild traumatic brain injuries occur at a brain von Mises stress of 20kPa. Baumgartner and Willinger^[41] observed that a brain von Mises stress of 18 kPa generates moderate neurological lesions which become severe from 38 kPa. Magnitudes of all the obtained coup and countercoup stresses are above 38 kPa. Therefore, all of the considered visco-hyperelastic models predict severe neurological lesions.

CONCLUSIONS

In the present research, a comparison is made among results of various (polynomial, Yeoh, Arruda–Boyce, and Ogden) visco-hyperelastic models that may be employed for simulation of the traumatic brain injuries, for the first time. CATIA geometry modeling, HYPERMESH and ANSYS finite element modeling, and LS-DYNA nonlinear dynamic

finite element analysis computer codes are employed in the present research. A pair of experimental results is employed to evaluate the accuracy of the resulting peak pressures and accelerations of the center of gravity of the brain predicted by the mentioned four visco-hyperelastic models. Comparing with both experimental results confirm that employing Arruda–Boyce or Ogden models may lead to inaccurate or even erroneous results. Comparisons made with the experimental results of accelerations of the center of gravity of the brain and pressure results of the coup and countercoup regions have led to an identical conclusion that the models may be ordered with respect to the accuracy as the polynomial, Yeoh, Arruda–Boyce, and Ogden models.

Financial support and sponsorship

Nil.

Conflicts of interest

There are no conflicts of interest.

REFERENCES

- Dawodu ST. Traumatic brain injury: Definition, epidemiology, pathophysiology, E Medicine from WebMD; 2007. Available form: <https://emedicine.medscape.com/article/326510-overview>. [Last Retrieved on 2017 Aug 16].
- El Sayed T, Mota A, Fraternali F, Ortiz M. Biomechanics of traumatic brain injury. *Comput Methods Appl Mech Eng* 2008;197:4692-701.
- Johnson E, Young P. The Analysis of Pressure Response in Head Injury. SAE Technical Paper; 2006.
- Yue X, Wang L, Sun S, Tong L. Viscoelastic finite-element analysis of human skull-dura mater system as intracranial pressure changing. *Afr J Biotechnol* 2008;7:689-95.
- Yue X, Wang L, Zhou F. Finite Element Analysis on Strains of Viscoelastic Human Skull and Duramater. Croatia: INTECH Open Access Publisher; 2010.
- Odgaard A. Three-dimensional methods for quantification of cancellous bone architecture. *Bone* 1997;20:315-28.
- van Noort R, Black MM, Martin TR, Meanley S. A study of the uniaxial mechanical properties of human dura mater preserved in glycerol. *Biomaterials* 1981;2:41-5.
- Willinger R, Kang H, Diaw B. Development and validation of a human head mechanical model. *Comptes Rendus de l'Académie des Sciences - Series IIB - Mechanics-Physics-Astronomy* 1999;327:125-31.
- Ding Z, Song D, Li S. Creep behavior of dura and substitutes. *J Shanghai Jiaotong Univ Chin Ed* 1998;32:93-6.
- Zhang L, Yang KH, Dwarampudi R, Omori K, Li T, Chang K, *et al.* Recent advances in brain injury research: A new human head model development and validation. *Stapp Car Crash J* 2001;45:369-94.
- Willinger R, Kang HS, Diaw B. Three-dimensional human head finite-element model validation against two experimental impacts. *Ann Biomed Eng* 1999;27:403-10.
- Kleiven S, von Holst H. Consequences of head size following trauma to the human head. *J Biomech* 2002;35:153-60.
- Horgan TJ, Gilchrist MD. Influence of FE model variability in predicting brain motion and intracranial pressure changes in head impact simulations. *Int J Crashworthiness* 2004;9:401-18.
- Liu S, Yin Z, Zhao H, Yang G. Investigation of the cavitation and pressure change of brain tissue based on a transparent head model in its decelerating impact. *J Mech Med Biol* 2010;10:361-72.
- Chen Y, Ostojic-Starzewski M. MRI-based finite element modeling of head trauma: Spherically focusing shear waves. *Acta Mech* 2010;213:155-67.
- Bergström J, Boyce M. Constitutive modeling of the time-dependent and cyclic loading of elastomers and application to soft biological tissues. *Mech Mater* 2001;33:523-30.

17. Brands DW, Peters GW, Bovendeerd PH. Design and numerical implementation of a 3-D non-linear viscoelastic constitutive model for brain tissue during impact. *J Biomech* 2004;37:127-34.
18. Franceschini G, Bigoni D, Regitnig P, Holzapfel GA. Brain tissue deforms similarly to filled elastomers and follows consolidation theory. *J Mech Phys Solids* 2006;54:2592-620.
19. Gasser TC, Holzapfel GA. A rate-independent elastoplastic constitutive model for biological fiber-reinforced composites at finite strains: Continuum basis, algorithmic formulation and finite element implementation. *Comput Mech* 2002;29:340-60.
20. Meaney DF. Relationship between structural modeling and hyperelastic material behavior: Application to CNS white matter. *Biomech Model Mechanobiol* 2003;1:279-93.
21. Miller K, Chinzei K. Mechanical properties of brain tissue in tension. *J Biomech* 2002;35:483-90.
22. Velardi F, Fraternali F, Angelillo M. Anisotropic constitutive equations and experimental tensile behavior of brain tissue. *Biomech Model Mechanobiol* 2006;5:53-61.
23. Kaster T, Sack I, Samani A. Measurement of the hyperelastic properties of *ex vivo* brain tissue slices. *J Biomech* 2011;44:1158-63.
24. Post A, Hoshizaki B, Gilchrist MD. Finite element analysis of the effect of loading curve shape on brain injury predictors. *J Biomech* 2012;45:679-83.
25. Zhou C, Khalif T, King AI, editors. *New Model Comparing Impact Responses of the Homogeneous and Inhomogeneous Human Brain*. Proceedings: Stapp Car Crash Conference; Society of Automotive Engineers SAE; 1995.
26. Johnson K, Becker J. *The Whole Brain Atlas*. Available form: <http://www.med.harvard.edu/aanlib>, 2017.
27. Saba L. *Image Principles, Neck and the Brain*. Boca Raton: CRC Press; 2016.
28. Yeoh O. Some forms of the strain energy function for rubber. *Rubber Chemistry and Technology*. 1993; 66:754-71.
29. Liu Y, Kerdok AE, Howe RD. A nonlinear finite element model of soft tissue indentation. *Medical Simulation*. Berlin: Springer; 2004. p. 67-76.
30. Shariyat M. A double-superposition global-local theory for vibration and dynamic buckling analyses of viscoelastic composite/sandwich plates: A complex modulus approach. *Arch Appl Mech* 2011;81:1253-68.
31. Shariyat M. A nonlinear double-superposition global-local theory for dynamic buckling of imperfect viscoelastic composite/sandwich plates: A hierarchical constitutive model. *Compos Struct* 2011;93:1890-9.
32. Shariyat M. Nonlinear thermomechanical dynamic buckling analysis of imperfect viscoelastic composite/sandwich shells by a double-superposition global-local theory and various constitutive models. *Compos Struct* 2011;93:2833-43.
33. Ashrafi H, Shariyat M. A nano-indentation identification technique for viscoelastic constitutive characteristics of periodontal ligaments. *J Biomed Phys Eng* 2016;6:109-18.
34. Shariyat M, Hosseini SH. Eccentric impact analysis of pre-stressed composite sandwich plates with viscoelastic cores: A novel global-local theory and a refined contact law. *Compos Struct* 2014;117:333-45.
35. Nahum AM, Smith R, Ward CC. *Intracranial Pressure Dynamics During Head Impact*. SAE Technical Paper; 1977.
36. Trosseille X, Tarriere C, Lavaste F, Guillon F, Domont A. Development of a FEM of the Human Head According to a Specific Test Protocol. SAE Technical Paper; 1992.
37. Available form: <https://www.brocku.ca/abieducation/binder/English/chap2.html>. [Last Retrieved on 2015 Feb 09].
38. Hardy WN, Mason MJ, Foster CD, Shah CS, Kopacz JM, Yang KH, *et al*. A study of the response of the human cadaver head to impact. *Stapp Car Crash J* 2007;51:17-80.
39. Takhounts EG, Ridella SA, Hasija V, Tannous RE, Campbell JQ, Malone D, *et al*. Investigation of traumatic brain injuries using the next generation of simulated injury monitor (SIMon) finite element head model. *Stapp Car Crash J* 2008;52:1-31.
40. Zhou C, Kahlil T, Dragovic L. *Head Injury Assessment of a Real World Crash by Finite Element Modelling*. AGARD; 1996.
41. Baumgartner D, Willinger R. Numerical modeling of the human head under impact: New injury mechanisms and tolerance limits. In: Gilchrist MD, editor. *IUTAM Symposium on Impact Biomechanics: From Fundamental Insights to Applications*. Netherlands: Springer; 2005.